

San Jose, CA); CD1b, CD4, and CD8 (Bcd3.1, OKT4, and OKT8; American Type Culture Collection); CNPase (2',3'-cyclic nucleotide 3'-phosphodiesterase) and p75^{NTR} (p75 neurotrophin receptor) (Chemicon-Millipore, Billerica, MA); and CD163 (BD Pharmingen) and IgG controls (Sigma, St. Louis, MO). The anti-*M. leprae* specific antigen PGL-1 was provided by Patrick J. Brennan of the Department of Microbiology, Immunology, and Pathology of Colorado State University (Fort Collins, CO). CD16-phycocerythrin (PE)-conjugated, CD163-PE-conjugated, and CD209-fluorescein isothiocyanate (FITC)-conjugated (R&D Systems) antibodies and IgG2b-FITC-conjugated control isotype antibody (Caltag, Buckingham, United Kingdom) were used for flow cytometry. The human recombinant cytokines interleukin-4 (IL-4; Preprotech, Rocky Hill, NJ), IL-15 and IL-10 (R&D Systems), and gamma interferon (IFN- γ ; BD Pharmingen) were used for *in vitro* assays.

Human Schwann cells. ST8814 tumor cell line was established from malignant schwannomas (neurofibrosarcomas) from patients with neurofibromatosis type I and was generously donated by J. A. Flechter (Dana Farber Cancer Institute, Boston, MA). The cells were grown in RPMI 1640 medium (Invitrogen, Carlsbad, CA) supplemented with 100 U of penicillin/ml, 100 μ g of streptomycin/ml, 2 mM L-glutamine, and 10% fetal calf serum (HyClone) in a humidified CO₂ incubator at 37°C.

Primary human Schwann cells were generously provided by Patrick Wood of the Department of Neurological Surgery, Miami Project to Cure Paralysis, University of Miami Miller School of Medicine, Miami, FL, and prepared from nerve explants from adult human donors as described previously (4, 36). The purity of Schwann cells was evaluated by labeling with anti-p75^{NTR} antibody, which revealed >95% p75^{NTR}-positive cells. These highly purified Schwann cells were seeded on mouse laminin 1 (4 μ g/ml) coated flasks in Dulbecco modified Eagle medium supplemented with 100 U of penicillin/ml, 100 μ g of streptomycin/ml, 2 mM L-glutamine, and 10% fetal calf serum (HyClone) in a humidified CO₂ incubator at 37°C.

Immunoperoxidase labeling. Frozen tissue sections and human Schwann cells were fixed with normal horse serum before incubation with the monoclonal antibodies (MAbs) for 60 min, followed by incubation with biotinylated horse anti-mouse IgG for 30 min. The primary antibody was visualized by using the ABC Elite system (Vector Laboratories, Burlingame, CA), which uses avidin and biotin-peroxidase conjugate for signal amplification. The ABC reagent was incubated for 1 h, followed by addition of substrate (3-amino-9-ethylcarbazole) for 10 min. Slides were counterstained with hematoxylin and mounted in crystal mounting medium (Biomedica, Foster City, CA).

Two- and three-color immunofluorescence and confocal microscopy. Immunofluorescence was performed by serially incubating cryostat tissue sections with mouse anti-human MAbs of different isotypes, anti-CD14 (IgG1), anti-CD68 (IgG1), anti-CD209 (IgG2b), anti-CNPase (IgG1), anti-p75^{NTR} (IgG1), anti-PGL-1 (IgG3), and anti-CD163 (IgG1), followed by incubation with isotype-specific, fluorochrome (A488, A568, or A647)-labeled goat anti-mouse immunoglobulin antibodies (Molecular Probes, Carlsbad, CA). For CNPase and CD163 colocalization anti-CD163-PE-conjugated antibody was used. Controls included staining with isotype-matched antibodies as described previously (23). Nuclei were stained with DAPI (4',6'-diamidino-2-phenylindole). Double and triple immunofluorescence of peripheral nerve sections was examined by using a Leica-TCS-SP MP inverted single confocal laser-scanning and a two-photon laser microscope (Leica, Heidelberg, Germany) at the Advanced Microscopy/Spectroscopy Laboratory Macro-Scale Imaging Laboratory, California NanoSystems Institute, University of California at Los Angeles.

Cell surface immunofluorescence labeling. To minimize nonspecific binding, human Schwann cells were incubated with human serum in fluorescence-activated cell sorting (FACS) buffer (phosphate-buffered saline, 0.1% sodium azide, and 2% fetal bovine serum). The cells were then incubated with fluorescently labeled primary antibodies for 30 min, washed two times before fixing in 1% paraformaldehyde, and then acquired by using a FACSCalibur (BD Biosciences). The data analysis was performed using FlowJo software (Tree Star, Ashland, OR).

Binding and phagocytosis. For binding and phagocytosis assays, PKH26-labeled live *M. leprae* was generously donated by James L. Krahenbuhl of National Hansen's Disease Programs, Health Resources Service Administration, Baton Rouge, LA. *M. leprae* was maintained in the footpads of nude mice. Freshly harvested *M. leprae* treated with 0.1 N NaOH (10⁹) was labeled with a red fluorescent dye PKH26 as previously described (17). PKH26-labeled *M. leprae* was added at 4°C for 6 h in antibiotic-free medium. The cells were harvested, washed, and labeled with CD209-specific antibody. For blocking, the cells were pretreated with medium alone, an IgG2b isotype, or a CD209-specific antibody (BD Pharmingen) for 1 h at 4°C. For phagocytosis, we cultured cells with PKH26-labeled *M. leprae* (24 h) as described previously (16).

Regulation of CD209 expression. Human Schwann cells were cultured with recombinant IL-4 (100 ng/ml), IL-10 (10 ng/ml), IL-15 (300 ng/ml), or IFN- γ (100 U/ml) for 48 h and enriched as described above. The cells were incubated with specific CD209-FITC antibody, and cells were acquired by using a FACS-Calibur (BD Biosciences). The data analysis was performed using FlowJo software. IL-4 was added 48 h prior to PKH26-labeled *M. leprae* stimulation, and a binding assay was carried out as described above.

Real-time quantitative PCR (qPCR). Human Schwann cells were stimulated with cytokines as described above, and RNA was isolated and cDNA was synthesized as described previously (15). The CD209 primers were 5'-GGATACA AGAGCTTAGCAGGGTG-3' (forward) and 5'-GCGTGAAGGAGAGGAGT TGC-3' (reverse). The relative quantities of the gene tested per sample were calculated against the ribosomal protein, large, P0 mRNA (36B4) using the $\Delta\Delta C_T$ formula as previously described (21).

Total RNA was isolated from three AFB⁺ and three AFB⁻ nerve lesions, and cDNA was prepared as described previously (19). TaqMan gene expression assays for detection of IL-4, IL-10, IFN- γ , and GAPDH (glyceraldehyde-3-phosphate dehydrogenase; Applied Biosystems, Foster City, CA) were used for amplification by qPCR. The relative quantities of the gene tested per sample were calculated against the GAPDH mRNA using the $\Delta\Delta C_T$ formula as previously described (21).

Statistical analysis. Results are reported as pooled data from an entire series of experiments, and described as mean \pm the SEM. For data comparison, Student *t* test was used with statistical significance at *P* < 0.05.

RESULTS

Nerve damage morphology and detection of *M. leprae* components in pure neural leprosy. A hematoxylin-and-eosin (H&E) histological stain was used to analyze the morphology of the peripheral nerve specimens of pure neural leprosy. The distribution of inflammatory cells was found to be distinct between AFB⁺ and AFB⁻ samples. In the AFB⁻ nerve specimens, the inflammatory cells were distributed in an organized granuloma containing a core of macrophages surrounded by a mantle of lymphocytes. In these specimens, the nerve fibers were almost completely destroyed. In contrast, AFB⁺ nerve specimens were characterized by a disorganized granuloma containing foamy macrophages interspersed with lymphocytes distributed between the nerve fibers; however, the nerve architecture appeared to be preserved (Fig. 1A).

To analyze the T-cell populations in nerve specimens that are keys to the adaptive immune response, MAbs to CD4 and CD8 were used with immunoperoxidase. The microanatomic distribution of CD4⁺ and CD8⁺ T cells was strikingly different between the AFB⁺ and AFB⁻ specimens. In the AFB⁺ biopsy samples, CD4⁺ and CD8⁺ T cells were located in the same region in the inflammatory infiltrate and between the nerve fibers. However, in the AFB⁻ nerve specimens, CD4⁺ T cells were detected within the granuloma, while CD8⁺ cells were surrounding in the mantle region (Fig. 1A). To determine the nature of the local T-cell response, the Th2 (IL-4 and IL-10) and Th1 (IFN- γ) mRNA levels in the nerve biopsies were analyzed. RNA was isolated from AFB⁺ (*n* = 3) and AFB⁻ (*n* = 3) specimens, followed by cDNA synthesis and qPCR. IL-4 and IL-10 mRNA levels were upregulated in AFB⁺ versus AFB⁻ nerve lesions. IFN- γ mRNA levels are slightly upregulated in AFB⁻ versus AFB⁺ nerve lesions (Fig. 1B).

The distribution of DCs (CD1b) and tissue macrophages (CD209), key cells of the innate immune response, were analyzed in the leprosy nerve lesions (16, 23). The prevalence of CD1b⁺ DCs was also distinct in AFB⁺ versus AFB⁻ nerve specimens. CD1b⁺ cells were common in AFB⁻ nerve specimens but rare or absent in the AFB⁺ nerve specimens (Fig.

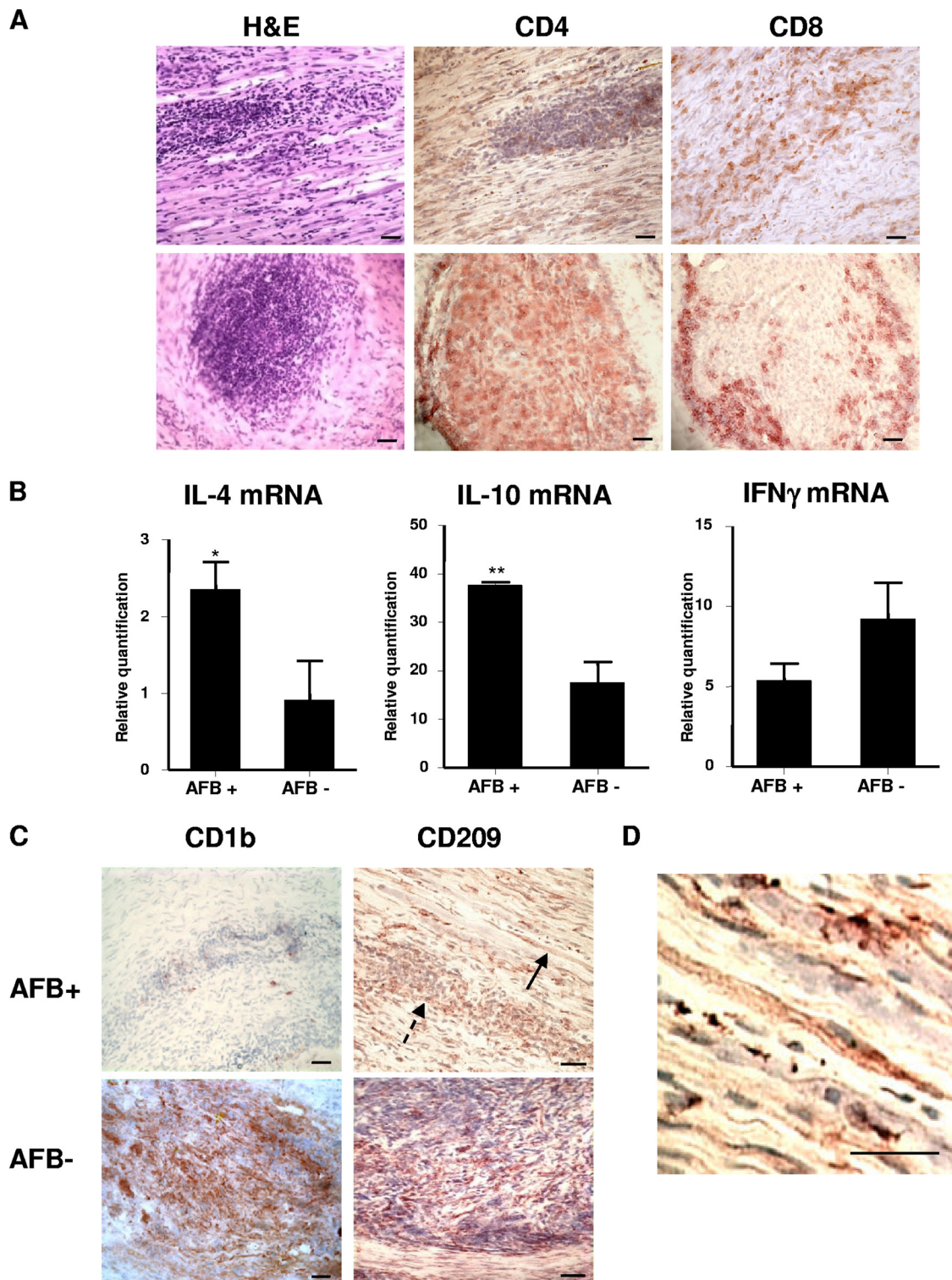


FIG. 1. Expression of CD209 in the peripheral nerve lesion; peripheral nerve tissue was labeled with MAbs using the immunoperoxidase method. (A) H&E was used for histology analysis (CD4 and CD8 [T cells]) in AFB⁺ and AFB⁻ nerve lesions. (B) Total mRNA was isolated from AFB⁺ (*n* = 3) and AFB⁻ (*n* = 3) nerve lesions, and the IL-4, IL-10, and IFN- γ mRNA levels were analyzed by TaqMan qPCR. **, *P* \leq 0.01; *, *P* \leq 0.05. (C) CD1b⁺ and CD209⁺ cells in AFB⁺ and AFB⁻ nerve lesions. A solid arrow indicates CD209⁺ cells with Schwann cell morphology, and a dashed arrow indicates CD209⁺ cells with macrophage morphology in an AFB⁺ nerve lesion. (D) Higher-magnification view of a CD209⁺ cell with Schwann cell morphology in an AFB⁺ nerve lesion. Bars, 40 μ m.

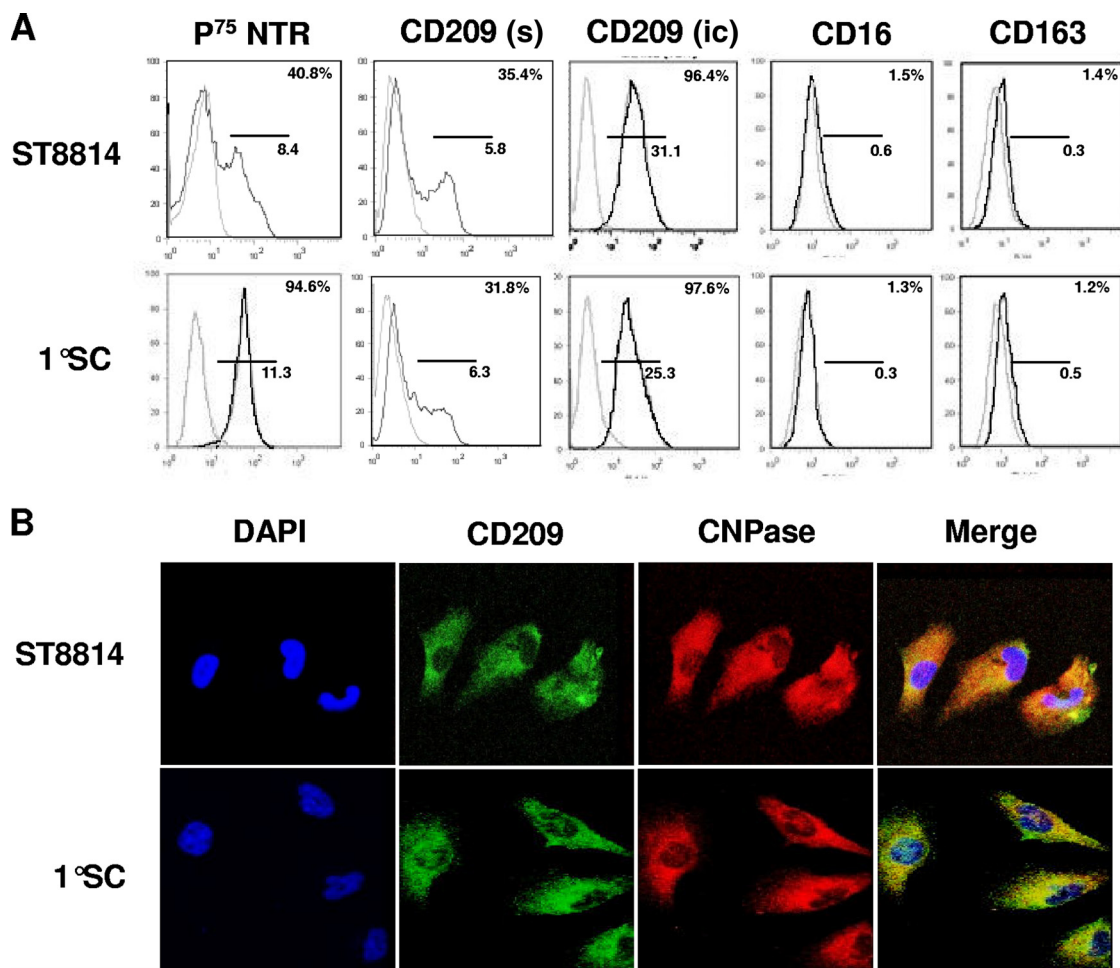


FIG. 2. Schwann cells express CD209 *in vitro*. (A) Human SCs (primary cells and ST8814) were collected; incubated with p75^{NTR}, CD209 surface (sc) and intracellular labeling (ic), and CD16 and CD163 antibodies as indicated; and analyzed by flow cytometry. (B) Human Schwann cells (primary cells and ST8814) were labeled with MAbs specific for CD209 and CNPase (Schwann cell marker). Confocal microscopy was used to detection of fluorescence. CD209 is visualized as green fluorescence, and *M. leprae* is visualized as red fluorescence. Nuclei were labeled with DAPI.

1C). CD209⁺ cells were detected on mononuclear cells in the inflammatory infiltrate in the nerve lesions, large ovoid cells typical of macrophage morphology (Fig. 1C, black dashed arrow). However, in these neural leprosy specimens, there were also CD209⁺ cells that did not have macrophage morphology. These CD209⁺ cells were characterized by an elongated shape and a spindle shaped nucleus, following the cell orientation, which is suggestive of a Schwann cell morphology (Fig. 1C, black bold arrow; Fig. 1D).

CD209 is expressed on Schwann cells and mediates the binding and uptake of *M. leprae*. To confirm that human Schwann cells express CD209, the ST8814 cell line and primary Schwann cell cultures were studied *in vitro*. The Schwann cell-specific marker, p75^{NTR}, was analyzed; ST8814 cells presented a medium expression of p75^{NTR} and primary cells showed a high expression of this marker, confirming the purity of this population. Approximately 30% of the Schwann cells, primary and cell line, expressed CD209 on the cell surface (Fig. 2A). For intracellular detection of CD209, cells were permeabilized before staining. Approximately 95% of Schwann cells ex-

pressed CD209 when intracellular staining was used (Fig. 2A). In addition, other macrophage markers, including CD16 and CD163, were not detected in human Schwann cells (Fig. 2A). Confocal microscopy was used to detect CD209 expression (green) in human Schwann cells (ST8814 and primary) identified by CNPase, a Schwann cell marker (red). The double-stained cells were identified by the colocalization (yellow) of CD209 and the Schwann cell marker, revealing the expression of CD209 on the surface and an apparent intracellular pattern (Fig. 2B).

CD209 has been shown to mediate the binding and uptake of viruses and bacteria, including mycobacteria, by immune cells. We were therefore interested in determining whether CD209 was involved in the binding and uptake of *M. leprae* by Schwann cells. Human Schwann cells, both the ST8814 line and primary Schwann cells, were cultured with live PKH26-labeled *M. leprae* at multiplicities of infection (MOIs) of 1:1, 10:1, and 50:1 for 6 h at 4°C, and binding was analyzed by flow cytometry. CD209⁺ Schwann cells were found to bind *M. leprae*, in particular at MOIs of 10:1 and 50:1 for both human

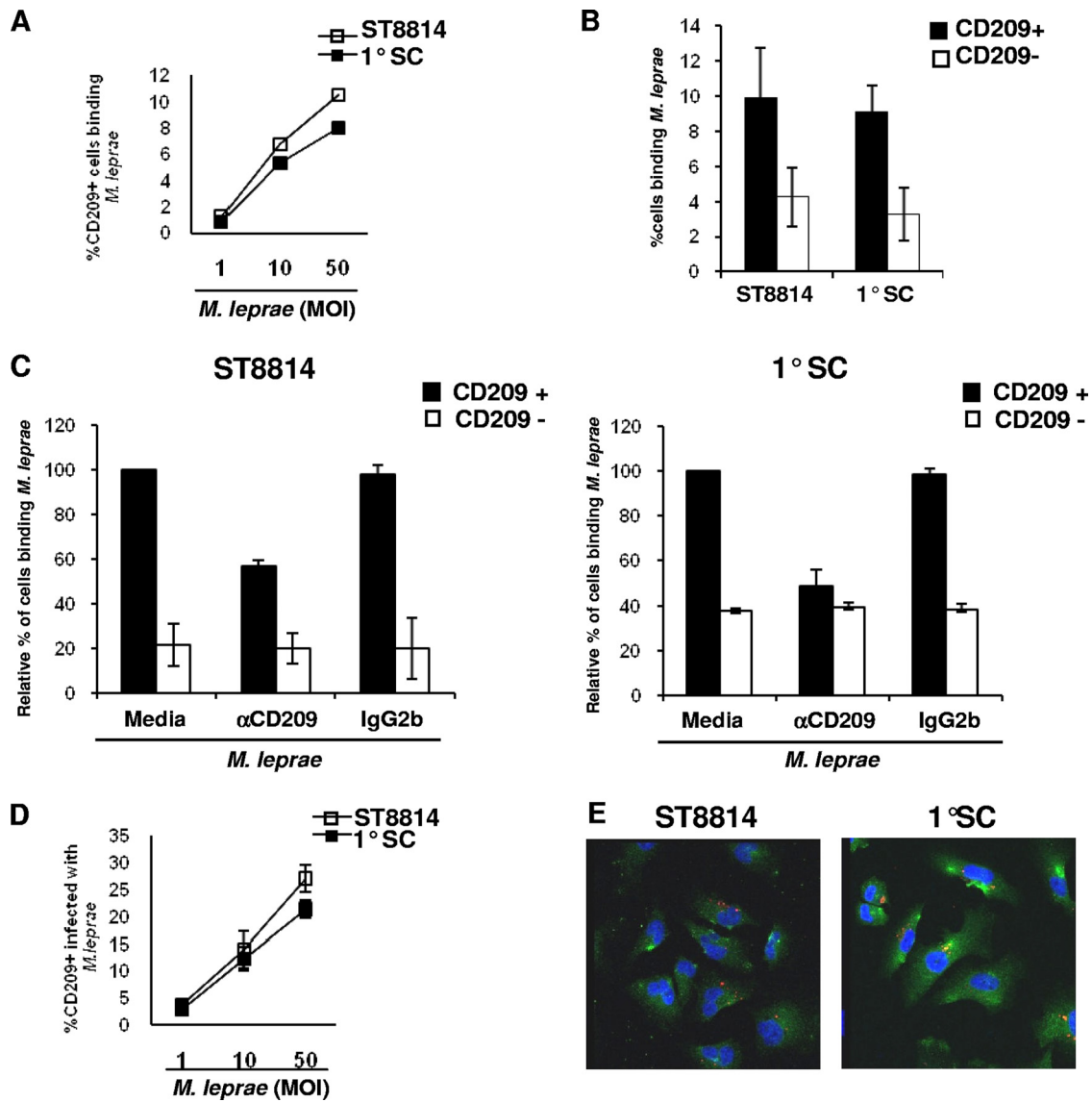


FIG. 3. CD209⁺ Schwann cells bind and uptake live *M. leprae* in vitro. (A) Human Schwann cells (ST8814 and primary cells) were incubated with live PKH26-labeled *M. leprae* (MOIs of 1:1, 10:1, and 50:1) for 6 h at 4°C. The data represent the percentage of double-positive cells for CD209⁺ cells and PKH26-labeled *M. leprae*, ST8814 cells (□) and primary cells (■). The data are representative of two individual experiments. (B) Comparison of *M. leprae* binding between CD209⁺ cells (■) and CD209⁻ cells (□). Binding was measured using an MOI of 10:1 for both human Schwann cells primary and ST8814. The Student *t* test was used for statistical analysis (*, *P* < 0.05). (C) Binding was measured in the presence of CD209 blocking antibody and control isotype. The data are represented as a percentage of the binding relative to the medium control in CD209⁺ cells in four individual experiments for ST8814 and three experiments for primary cells. Blocking was analyzed for CD209⁺ cells (■) and CD209⁻ cells (□). (D) Human Schwann cells (ST8814 and PSC) were cultured with PKH26-labeled *M. leprae* (MOIs of 1:1, 10:1, and 50:1) for 24 h at 33°C, and the uptake was measured by the double labeling. (E) Confocal images of *M. leprae*-infected CD209⁺ Schwann cells cultured as described in panel C. CD209 is visualized as green fluorescence, and *M. leprae* is visualized as red fluorescence. Nuclei were labeled with DAPI.

Schwann cell cultures (Fig. 3A). The ability of CD209⁺ and CD209⁻ cells to bind *M. leprae* (MOI of 10:1) was analyzed. The percentage of CD209⁺ cells binding *M. leprae* was significantly higher (*P* < 0.05) than that of CD209⁻ cells for both human Schwann cells types (ST8814 and primary cells) (Fig. 3B).

The role of CD209 in mediating the binding of *M. leprae* to ST8814 and primary Schwann cells was analyzed using an MOI of 10:1 in the presence or absence of an anti-CD209 blocking antibody or control isotype for 6 h at 4°C. Anti-CD209 blocked

M. leprae binding to Schwann cells by ca. 40% in both cell populations, whereas no blocking was observed with the isotype control. Meanwhile, the CD209 blocking antibody did not affect the binding of *M. leprae* by CD209⁻ Schwann cells (Fig. 3C). These data indicate that binding of *M. leprae* to Schwann cells involves CD209-dependent and -independent mechanisms.

To determine whether CD209⁺ Schwann cells can internalize live *M. leprae*, both primary Schwann cells and the ST8814 line were cultured with or without live PKH26-labeled *M. lep-*

rae (at MOIs of 1:1, 10:1 and 50:1) for 24 h at 33°C. We observed double positive cells, expressing both CD209 and *M. leprae*, particularly at MOIs of 10:1 and 50:1 (Fig. 3D). Together, these data indicate that *M. leprae* can infect human Schwann cells, with binding facilitated in some Schwann cell populations by CD209.

Cytokines induce CD209 expression in Schwann cells *in vitro*. The expression of CD209 on macrophages has been shown to be regulated by both Th1 and Th2 cytokines (16). Here, the ability of specific cytokines to regulate CD209 expression on Schwann cells was investigated. Both the ST8814 Schwann cell line and primary human Schwann cells were cultured with or without Th1 (IFN- γ and IL-15) and Th2 (IL-4 and IL-10) cytokines for 2 days at 37°C, and the expression of CD209 determined. Representative flow cytometry profiles (Fig. 4A) and mean of separate experiments (Fig. 4B) are shown. Treatment with IL-4 as well as IL-10 strongly upregulated CD209 expression by approximately 2 to 3-fold, and was significant both for CD209 MFI and the percentage of CD209⁺ cells versus media control ($P < 0.01$, Fig. 4B). For the primary Schwann cells, only IL-4 showed a significant increase in CD209 expression versus media control, slightly greater than 2-fold, both for MFI and the percentage of CD209⁺ cells ($P < 0.05$, Fig. 4B). IFN- γ had no effect on CD209 expression in the cultured Schwann cells. IL-15 slightly increased CD209 expression, both intensity and frequency, but the results were not statistically significant.

To determine whether the increase in CD209 expression was mediated at the level of transcription, Schwann cells were cultured with the recombinant cytokines for 24 h and RNA was isolated, followed by cDNA synthesis and qPCR. IL-4 and IL-10 induced CD209 mRNA in both the ST8814 and primary Schwann cell line, correlating with CD209 protein expression measured by flow cytometry (Fig. 4C).

To determine whether the ability of IL-4 to increase CD209 expression resulted in enhanced binding of *M. leprae* by CD209⁺ Schwann cells, ST8814 cells were cultured with or without IL-4 for 2 days prior to the addition of *M. leprae*. The binding assay was performed at 4°C for 4 h. Incubation with IL-4 significantly increased *M. leprae* binding in the Schwann cell line ST8814 by ca. 50% ($P < 0.05$, Fig. 4D). Therefore, the regulation of CD209 expression on Schwann cell by the local cytokine environment may influence binding to *M. leprae*, and subsequent uptake or infection.

CD209 is expressed by Schwann cells in nerve lesion of pure neural leprosy patients. The ability of CD209⁺ Schwann cells to bind and take up *M. leprae* prompted us to reexamine the nerve specimens to corroborate the *in vitro* findings with *in situ* evidence. To verify that CD209 was expressed on Schwann cells in lesions, CNPase was used as a specific Schwann cell marker. CD209 colocalized with CNPase in cells with Schwann cell morphology (Fig. 5A). In contrast, Schwann cells did not express another macrophage marker, the haptoglobin receptor CD163 (Fig. 5B).

The presence of *M. leprae* in the Schwann cells was investigated using a monoclonal antibody to PGL-1. Confocal laser microscopy revealed the colocalization within cells of Schwann cell morphology of the Schwann cell specific marker, CNPase, and the *M. leprae* marker PGL-1 (Fig. 5C). Therefore, we next determined the colocalization of PGL-1 with CD209⁺ cells,

focusing on cells with Schwann cell morphology (Fig. 5C). We detected colocalization of CD209 with the *M. leprae* PGL-1 in elongated cells. Finally, we were able to colocalize CNPase, CD209 and PGL-1 using triple confocal laser microscopy, as evidenced by the merge (white) of the three different colors CD209 (green), CNPase (cyan), and PGL-1 (red) (Fig. 5E). These data indicate the presence of *M. leprae* and/or its components in CD209⁺ Schwann cells *in situ*.

DISCUSSION

The C-type lectin, CD209 (DC-SIGN), has a key role in binding to microbial pathogens, facilitating their uptake by cells of the innate immune system (7). The expression of CD209 on tissue macrophages allows for uptake of and infection by mycobacteria, resulting in the destruction of the microbial invader by the host (16). Here we provide evidence that human Schwann cells express CD209, detected both *in vitro* in cultured Schwann cells and *in situ* in Schwann cells in neural leprosy lesions. CD209 partially mediated the ability of Schwann cells to bind to *M. leprae*, a key step in subsequent infection and consistent with the detection of *M. leprae* specific antigens both *in vitro* and *in situ* in CD209⁺ Schwann cells. CD209 was upregulated on Schwann cells by IL-4 but not IFN- γ , and facilitated binding to *M. leprae*. These data indicate that the regulated expression of CD209 provides a common mechanism by which macrophages and Schwann cells bind to and take up *M. leprae*.

C-type lectin receptors are typically expressed on myeloid DC and macrophages, key cells of the innate immune system. Examples of C-type lectins include the mannose receptor (CD206), expressed on macrophages and DCs, langerin (CD207), expressed especially by Langerhans cells, and collectins, such as mannose-binding lectin, SP-A, and SP-D, which can be produced by different cells and in different tissues (6, 37). Although initially CD209 was thought to be expressed on DCs, this was based on the study of monocyte-derived DC by culturing monocytes with granulocyte-macrophage colony-stimulating factor (GM-CSF) and IL-4 (28). However, CD209 is not detected on DCs in normal or disease tissues. Instead, CD209 is expressed by endothelial cells and tissue macrophages (16, 18, 29, 34). The present data extend the repertoire of CD209⁺ cells, providing evidence that human Schwann cells express C-type lectins. The expression of another C-type lectin, mannose receptor, was detected in rodent Schwann cells *in vitro*, and this can be related to the binding of mannose and mannosylated proteins (2). In addition, the human Schwann cell line ST8814 is able to take up mannosylated proteins, suggesting the presence of a C-type lectin receptor in these cells (3). These data support our results about CD209 expression on human Schwann cells.

The regulation of CD209 expression and its subsequent interaction with microbial pathogens can affect the induction of immune responses. Our data indicate that the Th2 cytokines, IL-4 and IL-10, upregulated CD209 expression in human Schwann cells *in vitro*, albeit only the experimental evidence indicating that IL-4 upregulates CD209 on primary human Schwann cells achieved statistical significance. Furthermore, IL-4-treated Schwann cells showed enhanced binding to *M. leprae*, the first step in the uptake of the pathogen. In contrast,

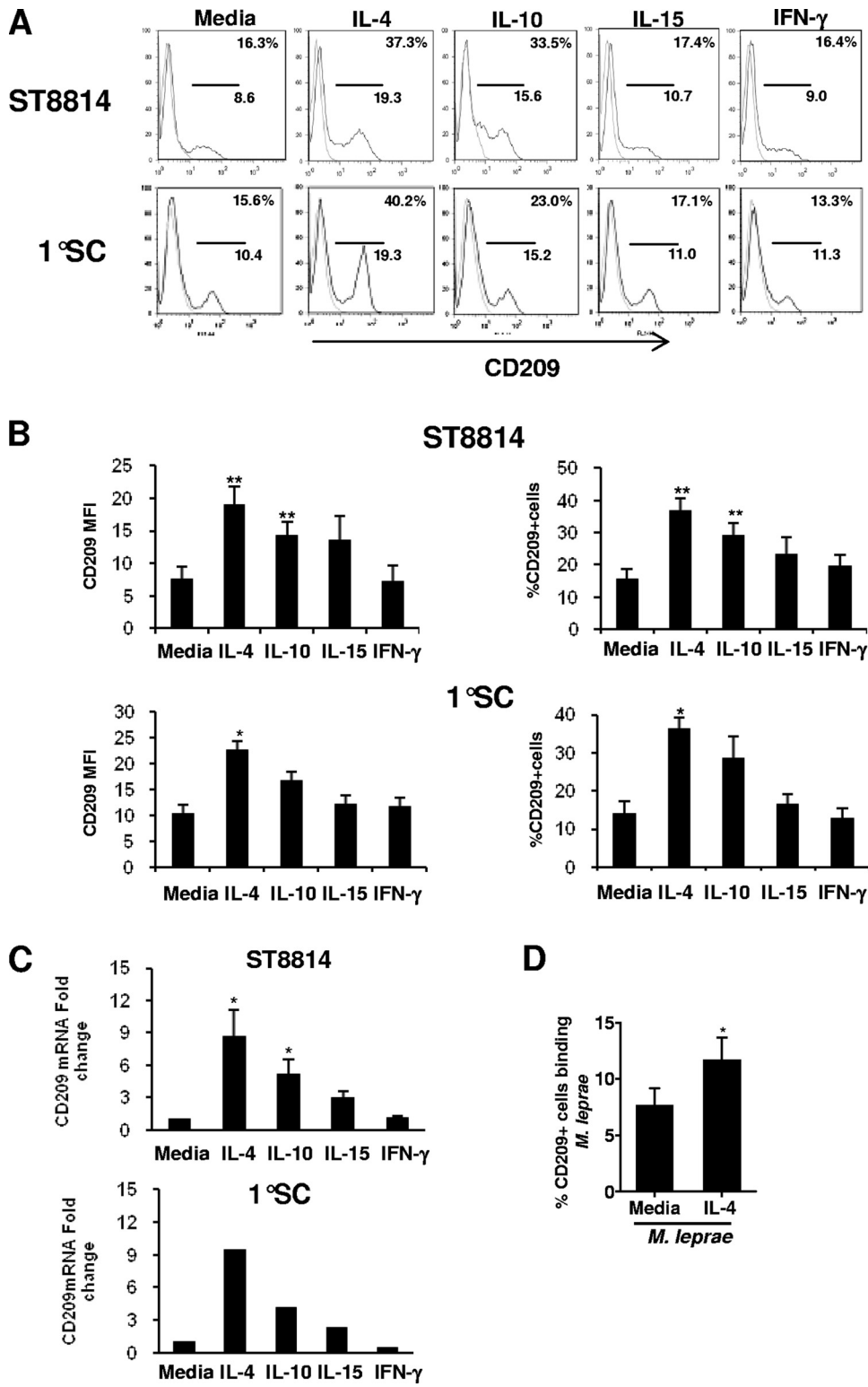


FIG. 4. Cytokines increase CD209 expression in human Schwann cells. Human Schwann cells were stimulated with IL-4, IL-10, IL-15, and IFN- γ for 2 days at 37°C. CD209 expression was measured by flow cytometry. The data are represented as the fluorescence intensity (Δ MFI) and the percentage of CD209⁺ cells. Six experiments were performed with the ST8814 cell line (A and B), and three experiments were performed with primary Schwann cells (A and B). (C) Schwann cells were stimulated with IL-4, IL-10, IL-15, and IFN- γ for 24 h; RNA was collected, and the CD209 message was analyzed by qPCR. The data represent the results of four experiments for ST8814 cells and two experiments for primary cells. (D) *M. leprae* binding was measured in Schwann cells (ST8814) stimulated or not with IL-4 as described for panel C. The data represent the percent binding relative to the medium control from three experiments. A Student *t* test was used for statistical analysis (**, $P < 0.01$; *, $P < 0.05$).

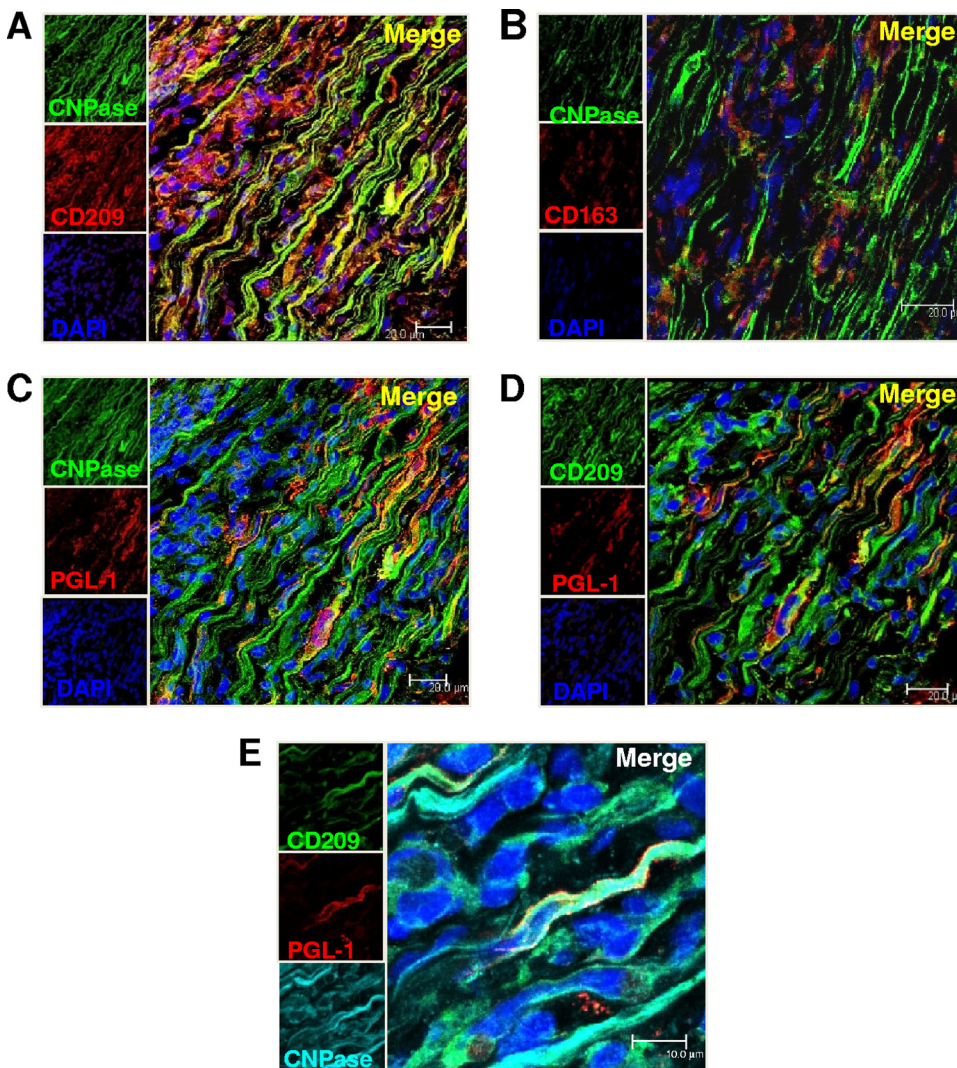


FIG. 5. CD209⁺ Schwann cells colocalize with *M. leprae* antigens in the nerve lesion. Peripheral nerve tissue was labeled with antibodies for the Schwann cell-specific marker CNPase and CD163 and CD209 and visualized by confocal laser microscopy. CNPase colocalizes with CD209 (A) but does not colocalize with CD163 (B). Nuclei were labeled with DAPI (blue). Peripheral nerve tissue was labeled with CNPase, CD209, and anti-*M. leprae* antigens (PGL-1) and visualized by confocal laser microscopy. CNPase (C) and CD209⁺ cells (D) colocalize with PGL-1. (E) Colocalization of CD209 (green), PGL1 (red), and CNPase (cyan). Nuclei were labeled with DAPI (blue images).

the Th1 cytokines, IFN- γ and IL-15, did not significantly affect Schwann cell expression of CD209. Therefore, the regulated expression of CD209 on Schwann cells by the local cytokine environment can facilitate infection by *M. leprae*, perhaps leading to subsequent tissue injury. IL-4 has also been found to induce CD209 on macrophages (28), providing a common mechanism by which macrophages and Schwann cells can bind to and take up mycobacteria.

The ability of CD209 to facilitate Schwann cell binding and phagocytosis of *M. leprae* is consistent with its known function on other cell types, including IL-15-derived macrophages and GM-CSF+IL-4-derived DCs (9, 16). CD209 recognizes specific mannose residues from mycobacteria, including *M. leprae* and *M. tuberculosis* (9, 11). Our results indicate that CD209 expression on Schwann cells is involved in the binding to *M. leprae*. Based on previous studies, it is likely that CD209 is interacting with Man-LAM (i.e., mannose-capped lipoarabino-

mannan) present in the *M. leprae* cell wall (9, 30). In addition to recognizing mycobacteria, CD209 recognizes HIV and may contribute to AIDS pathogenesis, including HIV infection of peripheral nerve Schwann cells (13, 31). Although *M. leprae* was taken up by CD209⁺ Schwann cells in a CD209-dependent manner, the pathogen was also taken up by CD209⁻ Schwann cells, indicating that multiple receptors are involved in binding and uptake (24). The unique tropism of *M. leprae* for Schwann cells is also facilitated by the ability of *M. leprae* PGL-1 to bind laminin 2 and subsequently bind and activate ERBB2 receptor, inducing the proliferation and demyelination of Schwann cells (26, 27, 36).

The infection of Schwann cells by *M. leprae*, which our data suggest is facilitated by CD209, ultimately leads to demyelination of peripheral nerves in leprosy and subsequent nerve damage. The interaction between *M. leprae* and Schwann cells can also trigger a number of immune events. For example, the

ability of *M. leprae* to trigger TLR2 activation on Schwann cells results in inflammatory cytokine production, including IL-6, IL-8, tumor necrosis factor alpha, and transforming growth factor β , as well as inducing apoptosis (24, 25). Schwann cells express major histocompatibility complex (MHC) class II and accessory molecules, including ICAM-1, and are therefore able to present antigens to CD4⁺ T cells under inflammatory conditions (1, 10, 14). Of relevance, Schwann cells can process and present *M. leprae* antigens via MHC class II and activate CD4⁺ T cells *in vitro*, and antigen presentation to T cells can trigger further inflammation and tissue injury (5, 32, 33). Therefore, the ability of Schwann cells to trigger both innate and acquired T-cell immune responses also contributes to the pathogenesis of nerve damage in leprosy.

The regulated expression of CD209 on Schwann cells and macrophages provides a common mechanism by which *M. leprae* infects these distinct cell types, contributing to the pathogenesis of human leprosy. Although our results suggest that IL-4, by enhancing CD209 expression, facilitates the interaction between the pathogen *M. leprae* and Schwann cells, it remains unclear whether this interaction provides an advantage to the host. The ability of IL-15 to regulate CD209 expression on macrophages facilitates the uptake and subsequent killing of mycobacteria (16), indicating a role in host defense. In macrophages, the antimicrobial and phagocytic programs are distinctly regulated, perhaps limiting the number of organisms that can be taken up and efficiently killed (22). It remains to be determined whether Schwann cells can mount an antimicrobial response and/or whether the coordinated uptake of the pathogen by multiple receptors overwhelms the individual host cell antimicrobial response. Nevertheless, additional insight into the mechanisms by which *M. leprae* and Schwann cells interact provides a potential opportunity to intervene with the goal of limiting nerve injury in patients with the disease, still a major socioeconomic burden on those suffering from leprosy.

ACKNOWLEDGMENTS

We thank Patrick J. Brennan of Department of Microbiology, Immunology, and Pathology of Colorado State University (Fort Collins, CO) for the anti-*M. leprae* antibodies and Patrick Wood of the Miami Project to Cure Paralysis (Miami, FL) for the primary human Schwann cells donation. We also thank James L. Krahenbuhl of the National Hansen's Disease Programs (Baton Rouge, LA) for the live *M. leprae* and Matthew J. Schibler and Laurent Bentolila of the Advanced Microscopy/Spectroscopy Laboratory Macro-Scale Imaging Laboratory California NanoSystems Institute UCLA, Los Angeles.

This study was supported in part by NIH grants AI22553 and AI047868.

REFERENCES

- Armati, P. J., J. D. Pollard, and P. Gatenby. 1990. Rat and human Schwann cells *in vitro* can synthesize and express MHC molecules. *Muscle Nerve* 13:106–116.
- Baetas-da-Cruz, W., L. Alves, M. C. Pessolani, H. S. Barbosa, A. Régnier-Vigouroux, S. Corte-Real, and L. A. Cavalcante. 2009. Schwann cells express the macrophage mannose receptor and MHC class II: do they have a role in antigen presentation? *J. Peripher. Nerv. Syst.* 14:84–92.
- Baetas-da-Cruz, W., L. Alves, E. V. Guimaraes, A. Santos-Silva, M. C. Pessolani, H. S. Barbosa, S. Corte-Real, and L. A. Cavalcante. 2009. Efficient uptake of mannoseylated proteins by a human Schwann cell line. *Histol. Histopathol.* 24:1029–1034.
- Casella, G. T., R. P. Bunge, and P. M. Wood. 1996. Improved method for harvesting human Schwann cells from mature peripheral nerve and expansion *in vitro*. *Glia* 17:327–338.
- Ford, A. L., W. J. Britton, and P. J. Armati. 1993. Schwann cells are able to present exogenous mycobacterial hsp70 to antigen-specific T lymphocytes. *J. Neuroimmunol.* 43:151–159.
- Geijtenbeek, T. B., and S. I. Gringhuis. 2009. Signalling through C-type lectin receptors: shaping immune responses. *Nat. Rev. Immunol.* 9:465–479.
- Geijtenbeek, T. B., D. S. Kwon, R. Torensma, S. J. van Vliet, G. C. van Duijnhoven, J. Middel, I. L. Cornelissen, H. S. Nottet, V. N. KewalRamani, D. R. Littman, C. G. Figdor, and Y. van Kooyk. 2000. DC-SIGN, a dendritic cell-specific HIV-1-binding protein that enhances trans-infection of T cells. *Cell* 100:587–597.
- Geijtenbeek, T. B., R. Torensma, S. J. Van Vliet, G. C. van Duijnhoven, G. J. Adema, Y. Van Kooyk, and C. G. Figdor. 2000. Identification of DC-SIGN, a novel dendritic cell-specific ICAM-3 receptor that supports primary immune responses. *Cell* 100:575–585.
- Geijtenbeek, T. B., S. J. Van Vliet, E. A. Koppel, M. Sanchez-Hernandez, C. M. Vandembroucke-Grauls, B. Appelmelk, and Y. Van Kooyk. 2003. Mycobacteria target DC-SIGN to suppress dendritic cell function. *J. Exp. Med.* 197:7–17.
- Gold, R., K. V. Toyka, and H. P. Hartung. 1995. Synergistic effect of IFN-gamma and TNF-alpha on expression of immune molecules and antigen presentation by Schwann cells. *Cell. Immunol.* 165:65–70.
- Gringhuis, S. I., J. den Dunnen, M. Litjens, H. B. van Het, K. Y. van, and T. B. Geijtenbeek. 2007. C-type lectin DC-SIGN modulates Toll-like receptor signaling via Raf-1 kinase-dependent acetylation of transcription factor NF- κ B. *Immunity.* 26:605–616.
- Jardim, M. R., S. L. Antunes, A. R. Santos, O. J. Nascimento, J. A. Nery, A. M. Sales, X. Illarramendi, N. Duppre, L. Chimelli, E. P. Sampaio, and E. P. Sarno. 2003. Criteria for diagnosis of pure neural leprosy. *J. Neurol.* 250:806–809.
- Keswani, S. C., M. Polley, C. A. Pardo, J. W. Griffin, J. C. McArthur, and A. Hoke. 2003. Schwann cell chemokine receptors mediate HIV-1 gp120 toxicity to sensory neurons. *Ann. Neurol.* 54:287–296.
- Koller, H., M. Schroeter, B. C. Kieseier, and H. P. Hartung. 2005. Chronic inflammatory demyelinating polyneuropathy: update on pathogenesis, diagnostic criteria and therapy. *Curr. Opin. Neurol.* 18:273–278.
- Krutzik, S. R., M. T. Ochoa, P. A. Sieling, S. Uematsu, Y. W. Ng, A. Legaspi, P. T. Liu, S. T. Cole, P. J. Godowski, Y. Maeda, E. N. Sarno, M. V. Norgard, P. J. Brennan, S. Akira, T. H. Rea, and R. L. Modlin. 2003. Activation and regulation of Toll-like receptors 2 and 1 in human leprosy. *Nat. Med.* 9:525–532.
- Krutzik, S. R., B. Tan, H. Li, M. T. Ochoa, P. T. Liu, S. E. Sharfstein, T. G. Graeber, P. A. Sieling, Y. J. Liu, T. H. Rea, B. R. Bloom, and R. L. Modlin. 2005. TLR activation triggers the rapid differentiation of monocytes into macrophages and dendritic cells. *Nat. Med.* 11:653–660.
- Lahiri, R., B. Randhawa, and J. L. Krahenbuhl. 2005. Effects of purification and fluorescent staining on viability of *Mycobacterium leprae*. *Int. J. Lepr. Other Mycobact. Dis.* 73:194–202.
- Lai, W. K., P. J. Sun, J. Zhang, A. Jennings, P. F. Lalor, S. Hubscher, J. A. McKeating, and D. H. Adams. 2006. Expression of DC-SIGN and DC-SIGNR on human sinusoidal endothelium: a role for capturing hepatitis C virus particles. *Am. J. Pathol.* 169:200–208.
- Lee, D. J., H. Li, M. T. Ochoa, M. Tanaka, R. J. Carbone, R. Damoiseaux, A. Burdick, E. N. Sarno, T. H. Rea, and R. L. Modlin. 2010. Integrated pathways for neutrophil recruitment and inflammation in leprosy. *J. Infect. Dis.* 201:558–569.
- Maeda, N., J. Nigou, J. L. Herrmann, M. Jackson, A. Amara, P. H. Lagrange, G. Puzo, B. Gicquel, and O. Neyrolles. 2003. The cell surface receptor DC-SIGN discriminates between *Mycobacterium* species through selective recognition of the mannose caps on liparabinomannan. *J. Biol. Chem.* 278:5513–5516.
- Monney, L., C. A. Sabatos, J. L. Gaglia, A. Ryu, H. Waldner, T. Chernova, S. Manning, E. A. Greenfield, A. J. Coyle, R. A. Sobel, G. J. Freeman, and V. K. Kuchroo. 2002. Th1-specific cell surface protein Tim-3 regulates macrophage activation and severity of an autoimmune disease. *Nature* 415:536–541.
- Montoya, D., D. Cruz, R. M. Teles, D. J. Lee, M. T. Ochoa, S. R. Krutzik, R. Chun, M. Schenk, X. Zhang, B. G. Ferguson, A. E. Burdick, E. N. Sarno, T. H. Rea, M. Hewison, J. S. Adams, G. Cheng, and R. L. Modlin. 2009. Divergence of macrophage phagocytic and antimicrobial programs in leprosy. *Cell Host. Microbe* 6:343–353.
- Ochoa, M. T., A. Loncaric, S. R. Krutzik, T. C. Becker, and R. L. Modlin. 2008. "Dermal dendritic cells" comprise two distinct populations: CD1⁺ dendritic cells and CD209⁺ macrophages. *J. Invest. Dermatol.* doi:10.1038/jid.2008.56.
- Oliveira, R. B., M. T. Ochoa, P. A. Sieling, T. H. Rea, A. Rambukkana, E. N. Sarno, and R. L. Modlin. 2003. Expression of Toll-like receptor 2 on human Schwann cells: a mechanism of nerve damage in leprosy. *Infect. Immun.* 71:1427–1433.
- Oliveira, R. B., E. P. Sampaio, F. Aarestrup, R. M. Teles, T. P. Silva, A. L. Oliveira, P. R. Antas, and E. N. Sarno. 2005. Cytokines and *Mycobacterium leprae* induce apoptosis in human Schwann cells. *J. Neuropathol. Exp. Neurol.* 64:882–890.

